

Simulation of Organic Chemical Movement in Hawaii Soils with PRZM: 1. Preliminary Results for Ethylene Dibromide¹

KEITH M. LOAGUE,² RICHARD E. GREEN,³ CLARK C. K. LIU⁴ AND TONY C. LIANG⁵

ABSTRACT: Leaching of agricultural chemicals to groundwater is an environmental issue of major concern in Hawaii. Fumigants used by the pineapple industry are a possible source of this contamination. In this paper we report the results of an initial evaluation of the Pesticide Root Zone Model (PRZM) for highly structured Hawaiian soils. We use PRZM to predict the transport of the soil fumigant ethylene dibromide (EDB) for two pineapple fields and compare the simulated concentration profiles with field measurements. Although preliminary, our results suggest that PRZM may be useful in the future for pesticide screening and risk assessment in Hawaii. The work reported here is part of a larger ongoing study concerned with development and application of methodology for assessing potential groundwater contamination by pesticides.

GROUNDWATER CONTAMINATION IS ONE of the nation's most important environment concerns (Pye and Patrick 1983, Sun 1986). The public's awareness of groundwater contamination has increased significantly in recent years because of well-publicized case histories such as Love Canal (Epstein et al. 1983).

In general, groundwater contamination occurs from either point or nonpoint sources. The failure of a waste management facility or a chemical spill are both examples of point sources. Applications of chemicals in agriculture and forestry (defoliants, herbicides, insecticides) constitute nonpoint sources.

The leaching of toxic chemicals, from either

point or nonpoint sources, to groundwater in certain hydrogeologic environments may take several years. This may lead to a false sense of environmental security for resource users and managers. However, the eventual detection of a pollutant in a groundwater system can easily result in staggering remedial action costs. The "wait and see" approach for a potential groundwater contamination problem is seldom acceptable. For this reason, dynamic simulation models that permit the user to ask "what if" questions are timely tools.

In this study, we report an evaluation of the Pesticide Root Zone Model (PRZM) for prediction of pesticide transport in highly structured Hawaiian soils. To place the relatively simple PRZM model in perspective, we present, in Appendix A, the partial differential equations that describe solute transport. Although preliminary, our results suggest that a modified version of PRZM may be useful in the future for pesticide screening and risk assessment in Hawaii. This investigation is only part of an ongoing interdisciplinary effort to limit groundwater contamination by toxic organic chemicals in Hawaii. The various activities included in our conceptual strategy are shown in Figure 1. The diagram indicates that regulatory activities such as pesticide registration and monitoring must be undergirded by objective analyses such as can

¹Manuscript accepted 18 March 1988. The work reported here was supported by EPA Cooperative Agreement CR811194-02-4, but the contents of this report do not necessarily reflect the views of the Agency and no official endorsement should be inferred.

²University of Hawaii at Manoa, Department of Geology and Geophysics, and Water Resources Research Center, Honolulu, Hawaii 96822. Current address: Department of Plant and Soil Biology, University of California, Berkeley, California 94720.

³University of Hawaii at Manoa, Department of Agronomy and Soil Science, Honolulu, Hawaii 96822.

⁴University of Hawaii at Manoa, Department of Civil Engineering, Honolulu, Hawaii 96822.

⁵University of Hawaii at Manoa, Department of Information and Computer Science, Honolulu, Hawaii 96822.

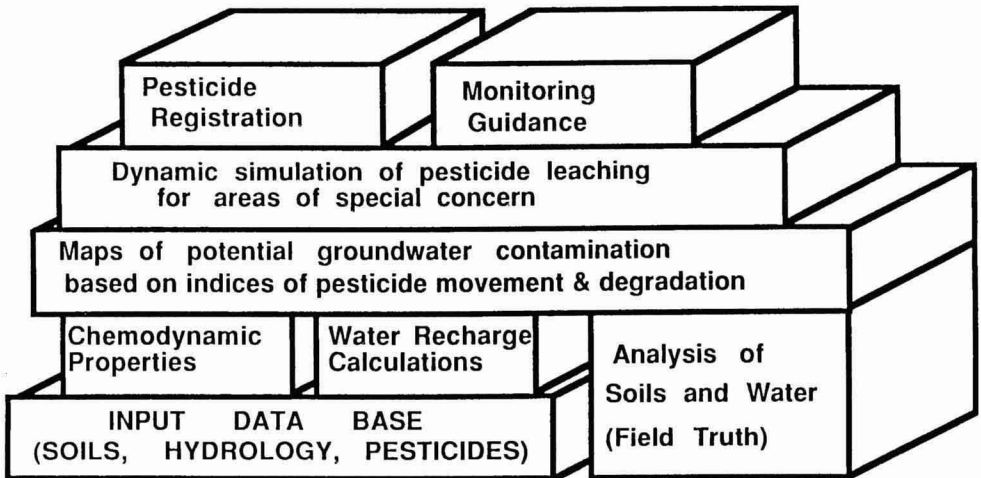


FIGURE 1. Strategy for reducing groundwater contamination by pesticides.

be provided by dynamic simulation and simple indices of pesticide movement and degradation. These assessment methodologies, in turn, depend upon a foundation of realistic data bases for soil properties, chemical properties, and rainfall/evapotranspiration, as well as measured environmental concentrations of contaminants (which we term "field truth") that can be used to evaluate modeling approaches.

PESTICIDE ROOT ZONE MODEL (PRZM)

The contamination of groundwater systems with agricultural pest control chemicals is an issue of concern for many in the United States. The U.S. Environmental Protection Agency (EPA) has long recognized the importance of this issue. EPA has aggressively attempted to identify existing problems, establish guidelines, and develop tools for engineering/management decisions related to nonpoint agricultural pollution. PRZM was developed by an interdisciplinary group of scientists in the EPA Environmental Research Laboratory in Athens, Georgia, to simulate the one-dimensional transport of a single pesticide within and at shallow depths below the unsaturated plant root zone.

Physically based solute-transport models usually are not practical tools due to data limitations. The creators of PRZM therefore elected to adopt less restrictive empirical procedures describing water movement in the interest of developing an operational procedure for leaching assessment. PRZM has three components: (1) a water-balance algorithm for the soil profile, (2) an erosion algorithm for the soil surface, and (3) a chemical-transport algorithm for the soil profile. Carsel et al. (1984) provide a complete description of PRZM. In the current study, the erosion component of PRZM was not utilized. Several components of PRZM related to our application are outlined below. A more comprehensive review of PRZM is given in Appendix B.

The water-balance algorithm is made up of three simple equations that partition water within and between the surface, the active root zone, and the remainder of the unsaturated zone. The elements of the water balance include precipitation, interception, evapotranspiration, runoff, and recharge. The water-balance calculations are performed on a daily time step.

Soil water recharge is the residual term in the PRZM water balance. The runoff calculation is therefore crucial to estimating how much water will infiltrate into the soil profile.

The empirical curve number scheme, popularized by the U.S. Soil Conservation Service (SCS), is used in PRZM to predict surface runoff. Once recharge is estimated, PRZM employs a set of simplistic "drainage rules" to predict soil moisture redistribution by one of two options.

In the first drainage option, water movement in the soil profile is assumed to be unrestricted. Two soil moisture parameters are needed: field capacity and wilting point. Field capacity is the value of soil water content when internal drainage has ceased. Under this free-drainage rule, soil water in excess of field capacity is routed to the next lower zone. The entire soil profile is assumed to drain excess water with every time step. Drainage under this rule is most probable for loose sandy soils of high conductivity. The wilting point is used as the lower limit to which plants can extract water from the soil matrix. The field capacity and wilting point concepts are both very subjective.

The second drainage option is designed to simulate water movement in soil profiles that contain layers of low conductivity. The interested reader is directed to Carsel et al. (1984) for a description of the method. Briefly, soil water redistribution is described for each layer in the profile by

$$\frac{\theta_i^{t+1} - \theta_i^{t_c}}{\theta_i - \theta_i^{t_c}} = \exp(-\lambda \Delta t) \quad (1)$$

where θ^{t+1} is soil water content at the end of the time step (dimensionless), θ^t is soil water content at the beginning of the time step (dimensionless), θ^{t_c} is soil water content at field capacity (dimensionless), i is the soil layer, λ is the drainage rate parameter (T^{-1}), and Δt is the time step (T). A disturbing property of this scheme is the possibility of exceeding saturated conditions for a low-conductivity layer when a more conductive layer is above it. If oversaturation occurs, PRZM redistributes water back into overlying layers.

The chemical-transport algorithm is an implicit finite-difference approximation to the one-dimensional advection–dispersion equation. Solution of the transport equation required values for soil water content and veloc-

ity throughout the soil profile at each time step. This information is obtained from the water-balance algorithm. However, because the water-balance calculations are not of the same rigor as the transport calculations, the concentration profiles predicted by PRZM are assumed to represent average field conditions and not point values. The form of the advection–dispersion equation employed by PRZM includes the effects of sorption, degradation, plant uptake, runoff, and erosion. In the current study, only the sorption component is utilized.

Pesticide soil interactions in the form of sorption and desorption are commonly described by the simple linear relationship $C_s = K_d \cdot C_w$, where C_s is the sorbed concentration of pesticides (dimensionless), C_w is the dissolved concentration of pesticides (ML^{-3}), and K_d is the sorption coefficient (L^3M^{-1}). The sorption coefficient is related to the soil organic carbon content by $K_d = K_{oc} \cdot f_{oc}$ (Green and Karickhoff 1988), where K_{oc} is the distribution coefficient for the chemical expressed on the basis of sorption per unit mass of organic carbon only, and f_{oc} is the fraction of organic carbon in the soil on a dry mass basis. The organic carbon-based distribution coefficient is taken as a constant.

Two of the major assumptions inherent to the proper application of PRZM are that: (1) drainage is free and (2) the dispersion coefficient is independent of soil water content, velocity, and depth. Table 1 summarizes how well PRZM stacks up against the physically based solute-transport model outlined in Appendix A. Based on its structure and underlying assumptions, PRZM is best suited to areas dominated by deep, well-drained sands where the water table is near the surface.

A number of researchers have evaluated PRZM under various environmental conditions (Bush et al. 1985; Carsel et al. 1985, 1986; Dean et al. 1984; Jones 1983; Jones et al. 1983; Melancon et al. 1986; J. Wagenet, personal communication, 1986). The objective of the current study was to perform a preliminary evaluation of how suitable PRZM is for fine-textured highly structured Hawaiian soils. For the work reported here PRZM was

TABLE 1
RELATIONSHIP BETWEEN PRZM AND PHYSICALLY BASED MODELS

DETERMINISTIC-CONCEPTUAL MODEL CHARACTERISTIC	PRZM	
	YES	NO
Three-dimensional representation		X
Coupled point solution		X
Flow component		
Physically based		X
Unsaturated	X	
Saturated		X
Transport component		
Physically based	X	
Unsaturated	X	
Saturated		X

deployed without modification. Khan and Green (1988) present the first Hawaiian application of PRZM in their report describing the interactive data input program "Pre-PRZM."

WATER AND SOIL CONTAMINATION ON OAHU

Groundwater contamination is of special concern for oceanic islands where an alternative source of water is not readily available. Saltwater encroachment caused by pumping is by far the biggest source of contamination for an island groundwater system. However, the leaching of agricultural chemicals to groundwater systems is increasingly becoming a major concern. Recent groundwater contamination discoveries in the State of Hawaii are chronicled by Oki and Giambelluca (1985) and by Lau and Mink (1987).

Several municipal wells on the island of Oahu were temporarily forced closed in the last few years by the discovery of trace concentrations of three potentially toxic chemicals: (1) dibromochloropropane (DBCP), (2) ethylene dibromide (EDB), and (3) trichloropropane (TCP). The wells pumping contaminated water all exploit the Pearl Harbor aquifer (Figure 2), which is the most important source of fresh water on Oahu. Fumigants used by the pineapple industry to control nematode populations during the last three decades are a possible source of the recent pollution. Both DBCP and EDB are soil

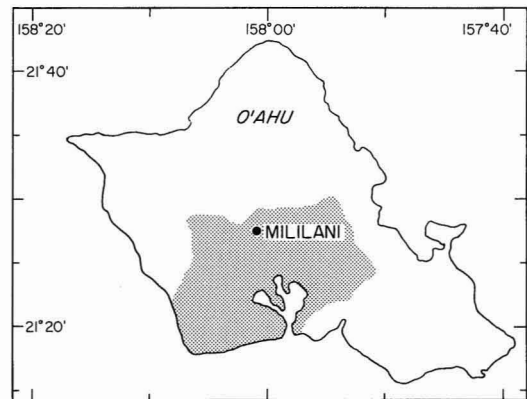


FIGURE 2. Location of Pearl Harbor aquifer on Oahu (indicated by stippled area).

fumigants, and TCP is an impurity of a third soil fumigant known as DD (a mixture of 1,3-dichloropropane and 1,2-dichloropropane). Prior to the recent discoveries, pesticides were not considered a threat to groundwater quality in Hawaii. The near-surface hydrogeologic environment appeared to preclude deep leaching of volatile nematicides.

In 1983, the Hawaii State Department of Agriculture conducted an extensive drilling and sampling program to identify which land-use activities had caused groundwater in Central Oahu to become contaminated with DBCP, EDB, and TCP (Wong 1983, 1987). In 1985, many of the 1983 sites were redrilled by the Water Resources Research Center at the

TABLE 2
GENERAL CHARACTERISTICS OF FIELDS 4201 AND 4213

	4201	4213
Location	21°29'5" N, 157°59'8" W	21°28'10" N, 157°59'58" W
Area (km ²)	0.8	0.6
Average elevation above sea level (m)	310	240
Average rainfall (m)	1.9	1.4
(Giambelluca et al. 1986)	(gauge 827)	(gauge 823)
Average pan evaporation (m)	1.3	1.7
(Ekern and Chang 1985)	(gauge 830.3)	(gauge 827)
Irrigation	None	None
Soil subgroup and series	Humoxic Tropohumults (Leilehua series)	Tropeptic Eustrtox (Wahiawa series)

University of Hawaii. Holes were drilled to greater depths, adjacent to the original holes, to confirm the earlier findings and track further pesticide movement (Peterson et al. 1985).

DATA BASE AND PARAMETER ESTIMATES

In this study, data from three of the twice-sampled sites are used to evaluate the performance of PRZM; the sites are identified as 4201a, 4201b, and 4213. We report EDB concentration profiles simulated with PRZM. EDB was selected for our initial study because only a single application had been made per field, and measured concentration profiles were obtained in both 1983 and 1985. In future investigations, we will include simulations of DBCP and TCP over many applications.

Pineapple fields 4201 and 4213 are located within the Pearl Harbor watershed near Mililani. General characteristics of the two fields are given in Table 2. A typical hydrogeologic cross section for the Mililani area is illustrated in Figure 3. The observed EDB concentration profiles for each of the three sites are shown in Figure 4. The base case parameters used to excite PRZM in this study are summarized in Table 3.

Daily rainfall and pan evaporation inputs for PRZM were estimated for this study from monthly data. Two simple schemes were used to convert the monthly information into daily

data: (1) monthly totals applied to the first day of the month and (2) monthly totals disaggregated equally to each day of the month. The daily time step, to which PRZM is restricted, appears to be appropriate for water-balance calculations in Hawaii (Giambelluca 1987, Giambelluca and Oki 1987).

The PRZM parameter λ , required in the second drainage option, was estimated for this study from soil water redistribution data reported by Green et al. (1982). Organic carbon

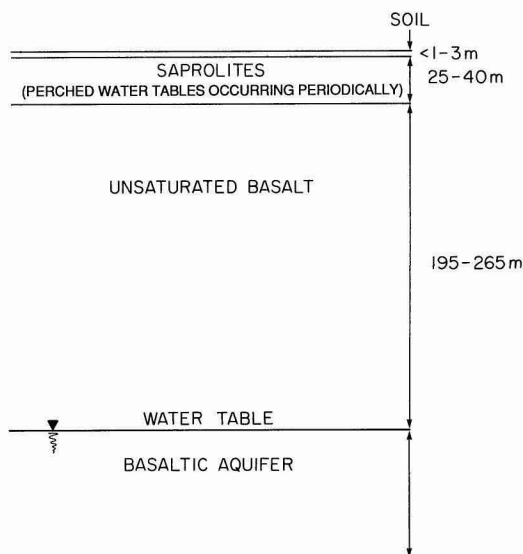


FIGURE 3. Generalized hydrogeological cross section for the Mililani area (after Or 1987).

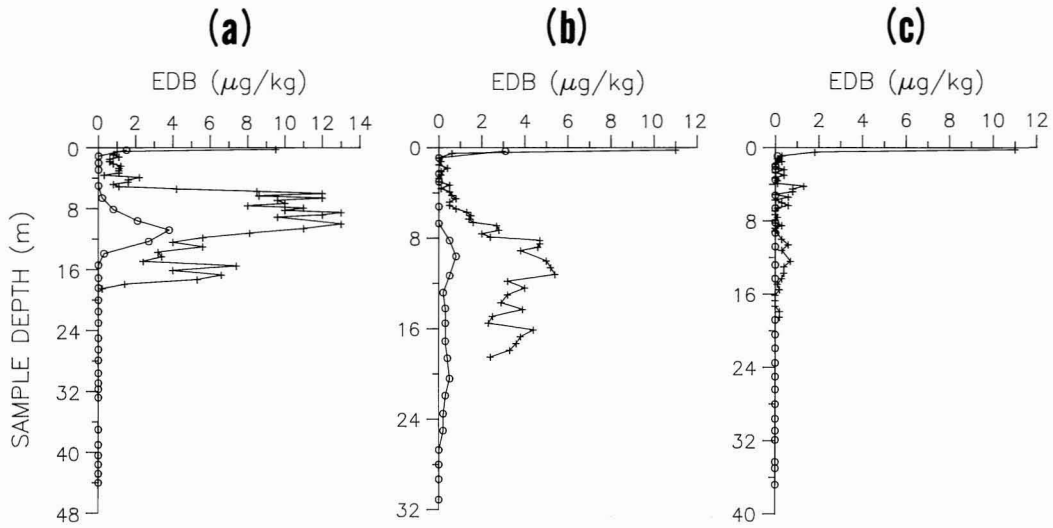


FIGURE 4. Observed EDB concentration profiles for (a) 4201a, (b) 420lb, and (c) 4213. The + and O represent 1983 and 1985 measurements, respectively.

TABLE 3
BASE CASE PARAMETERS (CASE A) FOR THE PRZM SIMULATIONS

PARAMETER/VARIABLE	4201a	4201b	4213	REFERENCE	CONFIDENCE
I. Climatology					
(1) Daily rainfall (mm) (based on representative areas; estimated from monthly rainfall)	Gauge 827	Gauge 827	Gauge 823	1, 4, 13	L
(2) Daily pan evaporation (mm) (based on representative areas; estimated from monthly pan evaporation; monthly means are not from the period of simulation)	Gauge 830.3	Gauge 830.3	Gauge 826	2	L
(3) Pan factor for evapotranspiration for pineapple (dimensionless)	0.2	0.2	0.2	3	M
(4) Minimum depth for evaporation (m)	0.30	0.30	0.30	4	M
II. Crop (pineapple)					
(1) Maximum root depth (m)	0.45	0.45	0.45	5	H
(2) Maximum area coverage (%)	95	95	95	5	H
(3) Maximum interception storage (mm)	1.3	1.3	1.3	6	M
(4) Planting data (month/year)	9/81	9/81	3/83	14	H
III. Hydrology					
(1) Runoff curve numbers (dimensionless)					
Crop	38	38	38	7	M
Residue	59	59	59	7	M
Fallow	80	80	80	7	M

TABLE 3 (continued)

IV. Management/pesticide					
(1) EDB application rate (kg·ha ⁻¹)	241	241	254	8, 9	H
(2) Application data (month/year)	9/81	9/81	3/83	14	H
(3) Incorporation depth (m)	0.30	0.30	0.30	8	H
(4) Plant uptake	Assumed to be 0			—	M
(5) Decay rate	Assumed to be 0			—	L
(6) Organic carbon distribution coefficient, K _{oc} (m ³ kg ⁻¹)	5.7 × 10 ⁻³	5.7 × 10 ⁻³	5.7 × 10 ⁻³	—	M
V. Soil					
(1) Organic carbon, oc(%)	Figure 5a	Figure 5b	Figure 5c	9	H
(2) Hydrodynamic dispersion, D (m ² sec ⁻¹)	1.5 × 10 ⁻⁸	1.5 × 10 ⁻⁸	1.5 × 10 ⁻⁸	10	M
(3) Bulk density (kg·m ⁻³)					
0.0–0.2 m	900	900	900	11	M
0.21–0.5 m	1080	1080	1080	11	M
0.51–20+ m	1270	1270	1270	11	L
(4) Soil water field capacity (dimensionless)	Assumed at 33 kPa				
0.0–0.2 m	0.31	0.31	0.31	11	M
0.21–0.5 m	0.40	0.40	0.40	11	M
0.51–20+ m	0.42	0.42	0.42	11	L
(5) Soil water wilting point (Dimensionless)	Assumed at 1.5 MPa				
0.0–0.2 m	0.25	0.25	0.25	12	L
0.21–0.5 m	0.25	0.25	0.25	12	L
0.51–20+ m	0.25	0.25	0.25	12	L
(6) Initial soil water content (dimensionless)	Estimated as midpoint between field capacity and wilting point			—	L

NOTE: H = high; M = moderate; L = low. References: (1) Division of Water and Land Development (1973); (2) Ekern and Chang (1985); (3) Ekern (1965); (4) T. Giambelluca, personal communication (1986); (5) D. Bartholomew, personal communication (1986); (6) P. Ekern, personal communication (1986); (7) Cooley and Lane (1982); (8) Wong (1983); (9) Peterson et al. (1985); (10) Khan and Green (1988); (11) Green et al. (1982); (12) U.S. Soil Conservation Service (1976); (13) Giambelluca et al. (1986); (14) L. Wong, personal communication (1986).

content profiles for the three sites are shown on Figure 5. The sole difference between the 4201a and 4201b parameter estimates in this study is the organic carbon information.

VOLATILIZATION-DEPENDENT INITIAL CONDITIONS

A major limitation of PRZM is the absence of a volatilization component. Volatilization is the process by which a compound evaporates in the vapor phase to the atmosphere. For some cases in this study we opt to simulate the vapor phase with a separate model (Green et al. 1986). Preprocessing short-term volatilization effects allowed us to better estimate realistic initial conditions. In the remainder of

this section we review the model used to simulate EDB volatilization.

EDB applied by shank injection is taken as a point source for two-dimensional simulation of residual concentrations. The governing equation for the initial phase simulations is

$$\frac{1}{R_L} D^P \left(\frac{\partial^2 C_w}{\partial x^2} + \frac{\partial^2 C_w}{\partial z^2} \right) - \kappa C_w = \frac{\partial C_w}{\partial t} \quad (2)$$

where

$$R_L = \rho_b K_d + \theta + n_a K_H \quad (\text{dimensionless}),$$

$$D^P = \frac{D^P}{R_L} \quad (\text{L}^2\text{T}^{-1}),$$

and D^P is effective diffusion coefficient (L^2T^{-1}), C_w is solute concentration in soil

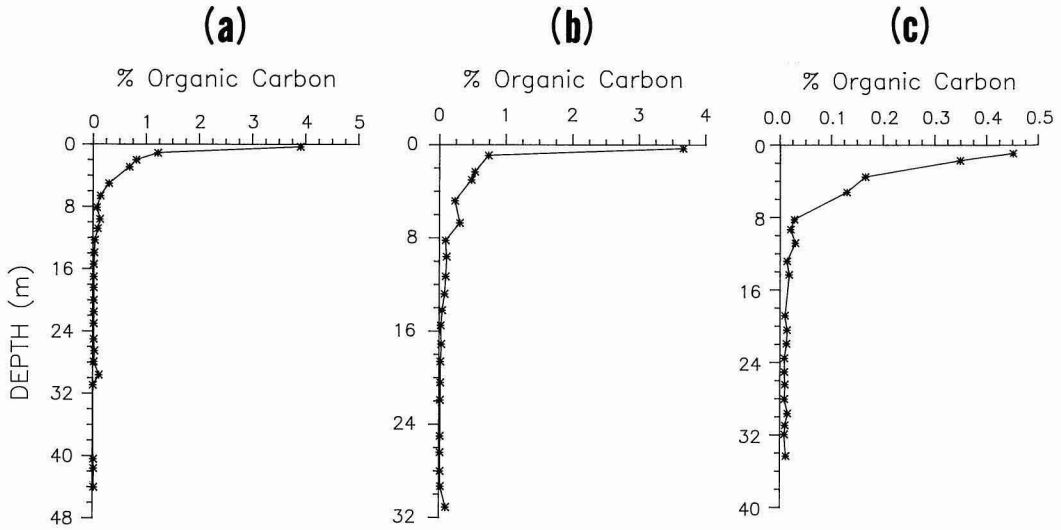


FIGURE 5. Observed organic carbon profiles for (a) 4201a, (b) 4201b, and (c) 4213. (Note the change in the concentration scale for 4213.)

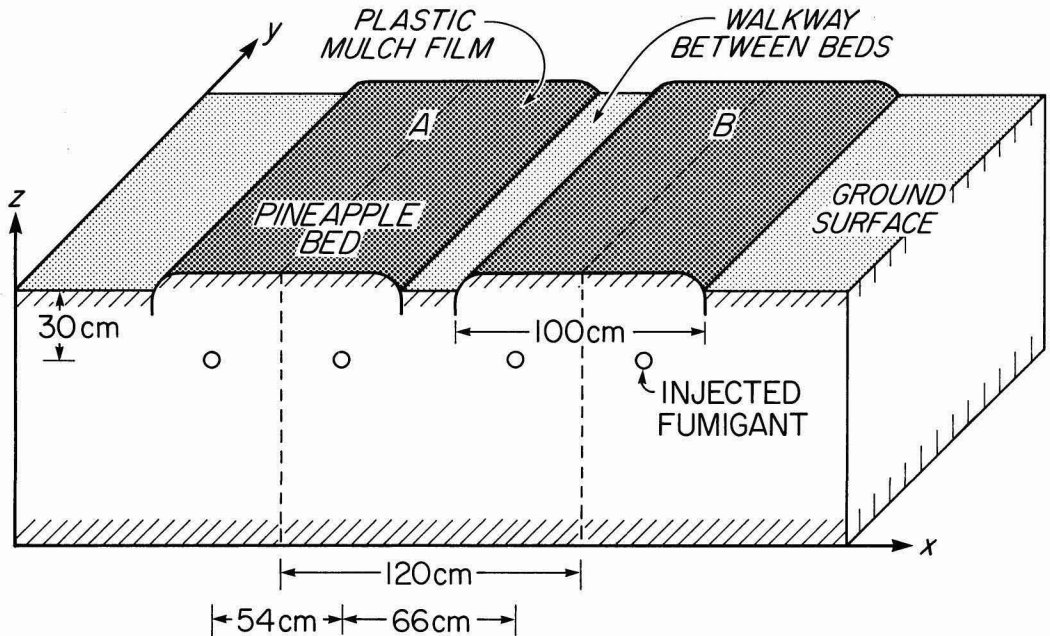


FIGURE 6. Cross-sectional geometry for two pineapple beds used for two-dimensional simulations of initial fumigant residual mixing. The area of simulation is between the bed centerlines A and B. The source zone for EDB is assumed to have the dimensions of the small rectangle. The bottom boundary is taken to be at 0.4 m.

solution (ML^{-3}), κ is decay coefficient (T^{-1}), ρ_b is bulk density (ML^{-3}), θ is soil water content (dimensionless), n_a is air-filled porosity (dimensionless), K_H is Henry's law constant (dimensionless), x , z are spatial coordinates, and t is time (T).

The initial conditions are $C_w = C_0$ for all points where the fumigant is applied and $C_w = 0$ for all other points. The boundary conditions are

$$\frac{\partial C_w}{\partial x} = 0 \quad \text{where } x = 0 \text{ for all } t$$

$$\frac{\partial C_w}{\partial x} = 0 \quad \text{where } x = 1 \text{ for all } t$$

$$\frac{\partial C_w}{\partial z} = 0 \quad \text{where } z = d \text{ for all } t$$

$$D' \frac{\partial C_w}{\partial z} = \frac{D_G^{\text{air}} C_w}{dR_G} \quad \text{where } z = 0 \text{ for the uncovered surface for all } t$$

Here,

$$R_G = \frac{\rho_b K_d}{K_H} + \frac{\theta}{K_H} + n_a \quad (\text{dimensionless})$$

l is distance between two consecutive application points (L), d is thickness of stagnant air layer above soil surface (L), and D_G^{air} is the vapor-air diffusion coefficient (L^2T^{-1}).

An explicit finite-difference scheme was used to solve equation (2). Processes other than volatilization, such as biodegradation and hydrolysis, which also reduce fumigant residuals, are lumped into the decay term. Figure 6 illustrates the cross-sectional geome-

try for the systems simulated in this study. We found that after 15 days a reasonably uniform fumigant residual distribution was achieved. Therefore, we used the average concentrations at the end of a given 15-day simulation with the two-dimensional initial-phase model as the initial concentrations for subsequent one-dimensional PRZM simulations. The parameters used for our volatilization simulations are given in Table 4.

NEAR-SURFACE SIMULATIONS

In this section, PRZM is used to predict EDB transport within the near-surface profile based on the 4201a data set. Only the top meter of the soil profile is used for the simulations discussed here. The results are intended to demonstrate how PRZM functions and to draw attention to a few nuances inherent to solute-transport modeling. Detailed field measurements of EDB concentrations were not available; therefore, comparison of observed and predicted profiles is not possible in this section.

Predicted EDB concentration profiles are shown in Figure 7 for various simulation scenarios. Each case is summarized in Table 5. The space increment (or element size) is set at 2 cm for all the near-surface simulations. The predicted 30-day concentration profiles for cases A–D are overlaid in Figure 8. The smearing effect of the dispersion coefficient is illustrated by comparing cases A and B. The consequence of free versus restricted drainage is shown by comparing cases A and C. The outcome of considering volatilization is dem-

TABLE 4

PARAMETER VALUES USED FOR THE CASE D VOLATILIZATION SIMULATIONS

PARAMETER	VALUE
Decay coefficient, κ (sec^{-1})	4.4×10^{-8}
Henry's law constant, K_H (dimensionless)	0.0148
Thickness of stagnant air layer above soil surface, d (m)	0.01
Effective diffusion coefficient, D^p ($\text{m}^2\text{sec}^{-1}$)	8.3×10^{-8}
Vapor-air diffusion coefficient, D_G^{air} ($\text{m}^2\text{sec}^{-1}$)	6.9×10^{-6}

(a)

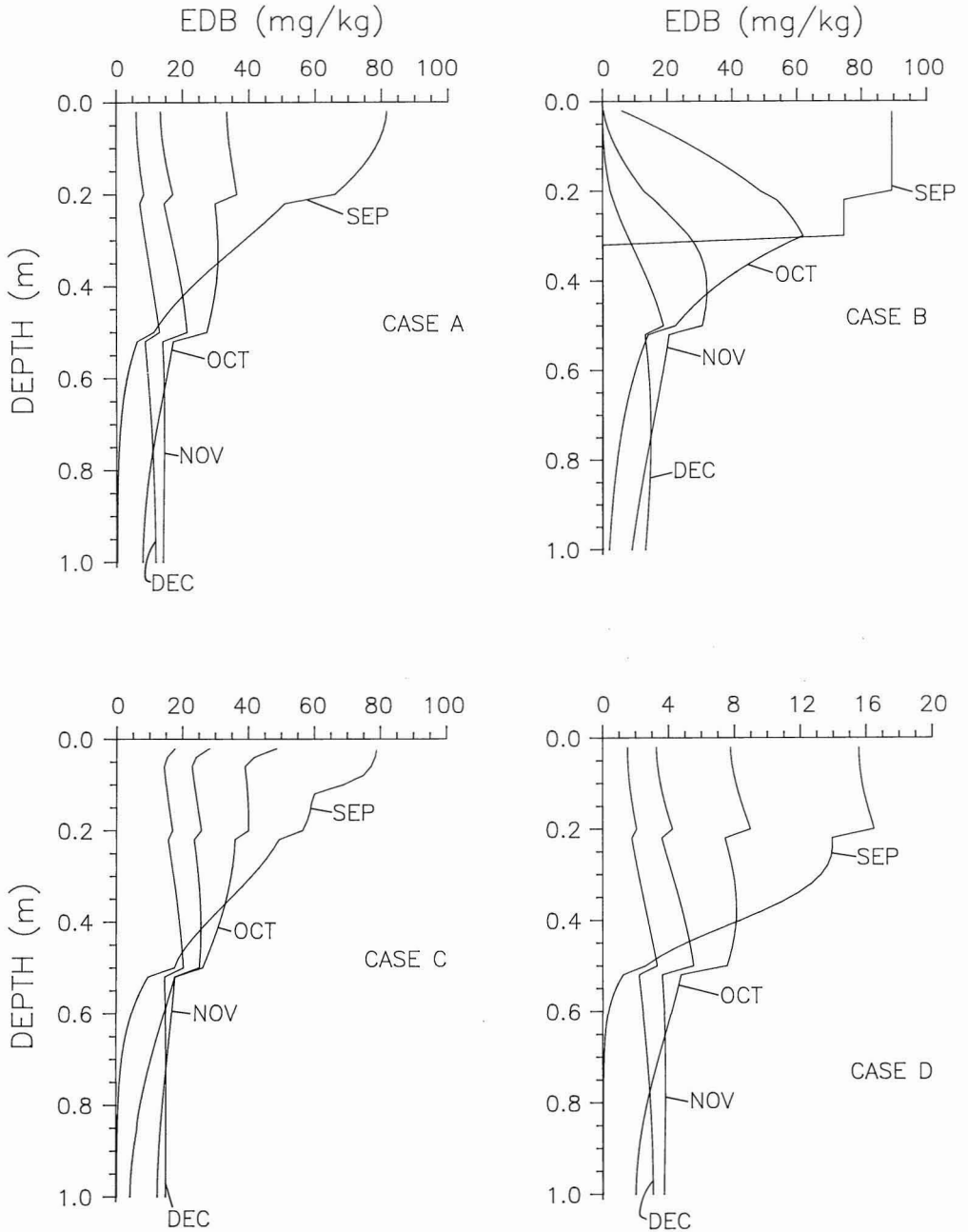


FIGURE 7. Predicted 1981 EDB concentration profiles for 4201a for (a) monthly rainfall (above) and (b) daily rainfall (facing page).

(b)

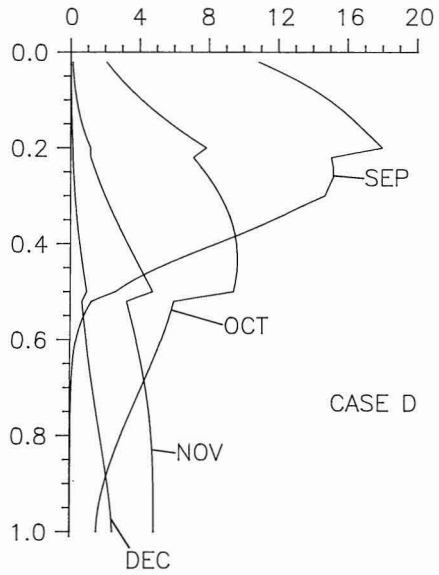
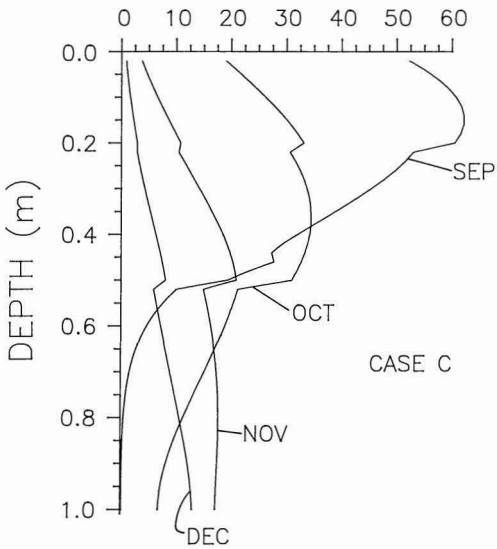
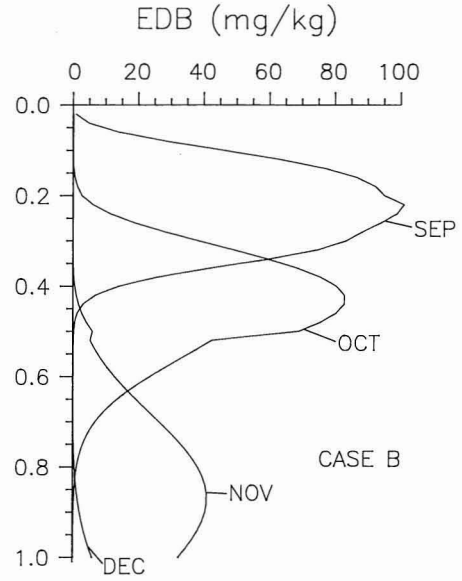
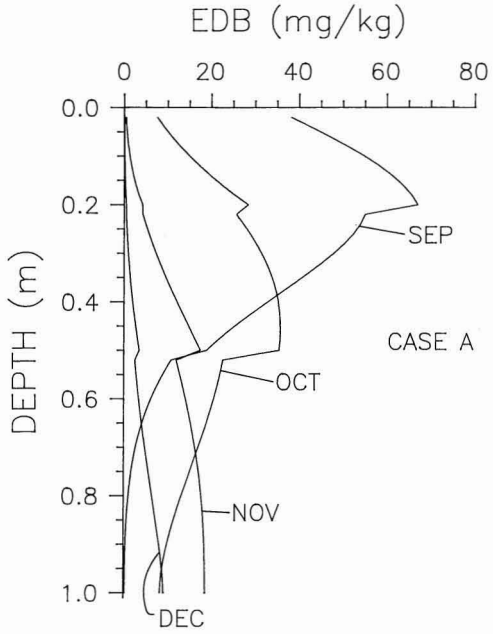


TABLE 5
ALTERNATIVE SIMULATION SCENARIOS FOR 4201a, 4201b, AND 4213

PARAMETER VALUES AND OPTIONS	CASE			
	A	B	C	D
D ($m^2 \text{sec}^{-1}$)	1.5×10^{-8}	0	1.5×10^{-8}	1.5×10^{-8}
EDB application ($\text{kg} \cdot \text{ha}^{-1}$)				
4201	241	241	241	241
4213	254	254	254	254
Drainage option*	a	a	b	a
Volatilization	No	No	No	Yes

NOTE: Case A corresponds to the base case summarized in Table 3.

* a = free; b = restricted.

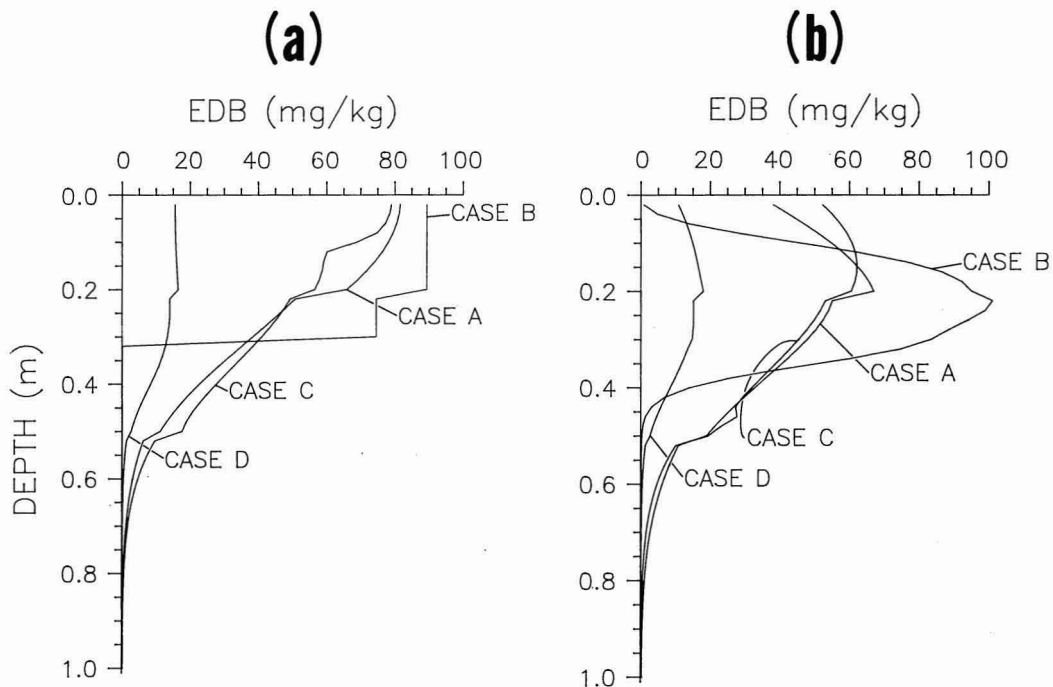


FIGURE 8. Composite overlays of predicted (1981) 30-day EDB concentration profiles for 4201a for (a) monthly rainfall and (b) daily rainfall.

onstrated by comparing cases A and D. The effect of different rainfall disaggregation schemes is seen by comparing parts a and b in both Figures 7 and 8. The cumulative pesticide flux past the maximum root depth for cases A–D is traced in Figure 9 for both disaggregation schemes.

Inspection of Figures 7–9 leads to the fol-

lowing observations:

(1) The near-surface simulations for cases A–D (Figures 7, 8) show that the daily rainfall disaggregation scheme results in smoother concentration profiles. The breaks in the traces are related to the changes in soil layer parameters.

(2) The cumulative EDB flux for the vari-

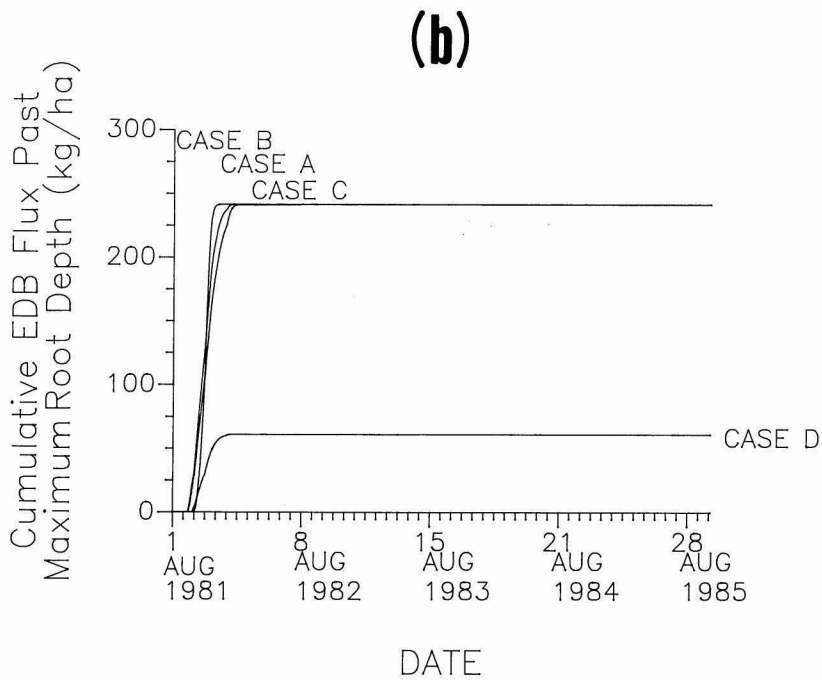
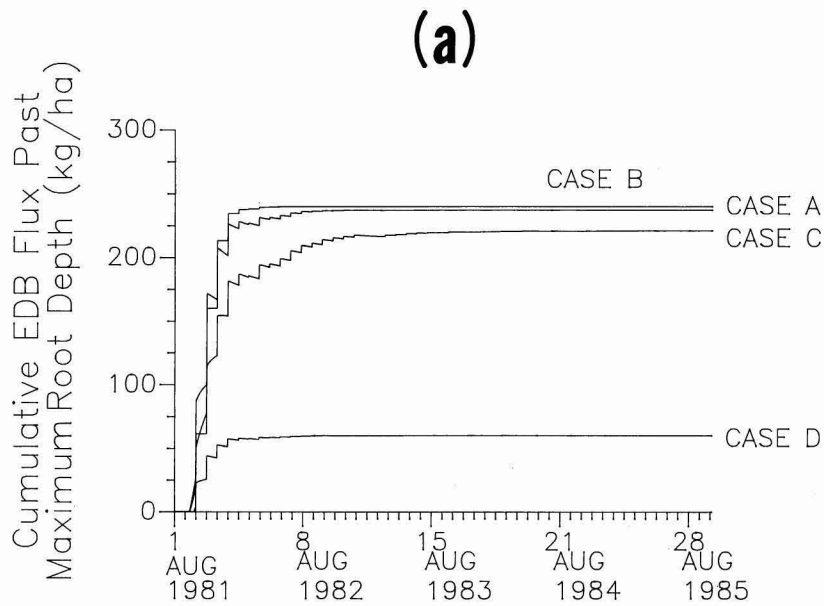


FIGURE 9. Simulated EDB flux for 4201a for (a) monthly rainfall and (b) daily rainfall.

ous simulation cases (Figure 9) illustrates that the pesticide is leached past the maximum root depth within months of application for daily rainfall disaggregation and that under monthly disaggregation transport is at a slower rate.

The effects of space increment (Δz) selection are well illustrated in Figure 10. For the small simulation depth, smoother concentration profiles result from smaller space increments. Carsel et al. (1984) suggest a 5-cm increment and a minimum of 30 elements. The results in Figures 7 and 8 are based on a 2-cm increment and 50 elements.

Numerical dispersion is usually of concern when a finite-difference approximation is made for the advection–dispersion equation (Anderson 1979). Numerical dispersion associated with changes in space increment are shown in Figure 10a. Physical dispersion, with

numerical dispersion included, represented by a suite of dispersion coefficients, is illustrated in Figure 10b. Carsel et al. (1984) provide guidelines to reduce the impact of numerical dispersion. One of their suggestions, setting the dispersion coefficient to 0, is conceptually disturbing. In effect, this amounts to assuming that physical dispersion is effectively approximated by numerical dispersion. There is no physical basis for this supposition.

PREDICTED EDB CONCENTRATION PROFILES

In this section, PRZM is used to predict observed EDB profiles for 4201a, 4201b, and 4213. The measured EDB concentrations for deep profiles described in the previous section present an opportunity to evaluate PRZM. We recognize that PRZM was not developed to

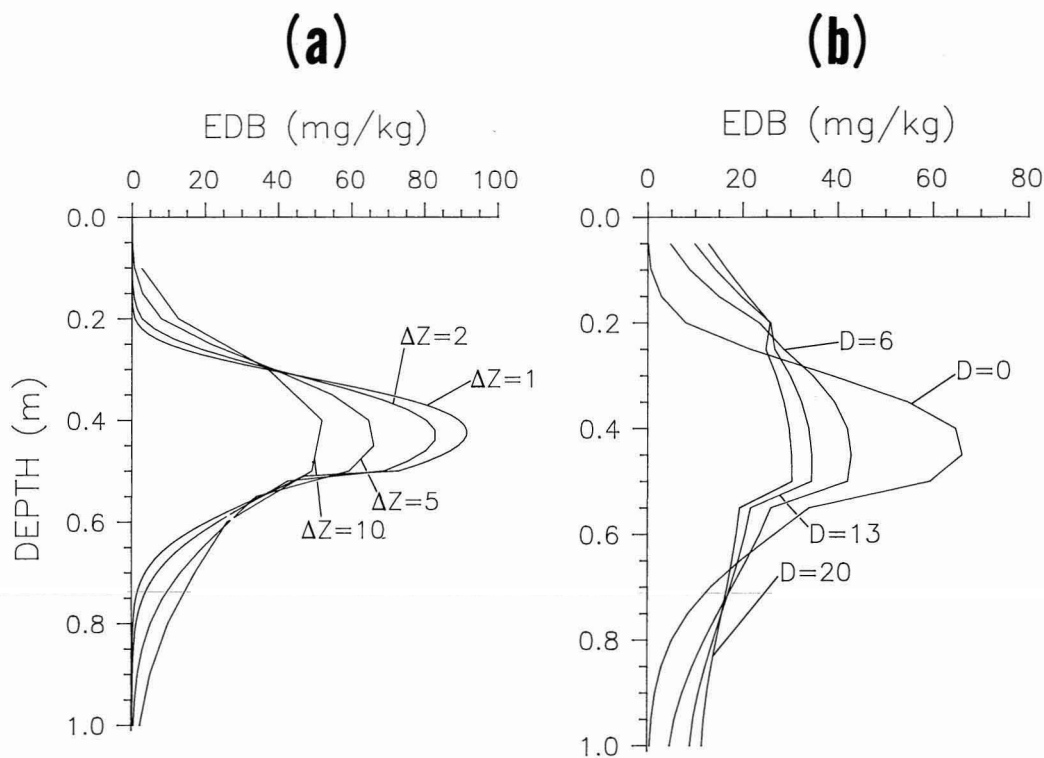


FIGURE 10. Numerical dispersion experiments for 4201a for October 1981 using the daily rainfall disaggregation scheme. (a) Changes in space increment (Δz , cm) with $D = 0$. (b) Changes in dispersion coefficient (D , $\text{cm}^2 \text{day}^{-1}$) with $\Delta z = 5$ cm.

simulate pesticide movement over the extended depths included in this study. However, with the model limitations in mind, we have applied PRZM beyond its intended range to determine whether it can provide reasonable estimates of the depth of the EDB peak concentration over a multiple-year period following application. We do not consider this exercise to constitute a rigorous test of PRZM.

PRZM-simulated water-balance summaries for pineapple fields 4201 and 4213 are shown on Figure 11. Predicted EDB concentration profiles for the base case (case A) for each of the three fields are shown on Figure 12. Predicted EDB concentration profiles for 4201a (case A) with $\pm 5\%$ rainfall are shown on Figure 13. Predicted EDB concentration profiles for the alternative simulation scenarios summarized in Table 5 are shown on Figure

14. Observed and predicted EDB concentration profiles for cases A–D for field 4201b are shown on Figure 15. The space increment is set at 10 cm for each of the deep profile simulations.

Inspection of Figures 11–15 leads to the following observations:

(1) The obvious difference between the two rainfall disaggregation schemes (Figure 11) for both the wet (4201) and dry (4213) fields is that the daily scheme results in more recharge and therefore faster and greater EDB transport (Figure 12). Khan and Green (1988) report that the movement of DBCP as predicted by PRZM for two Maui locations was deeper with the monthly disaggregation scheme. Those results are traceable to a reduction in recharge caused by higher evapotranspiration rates under the daily disaggregation

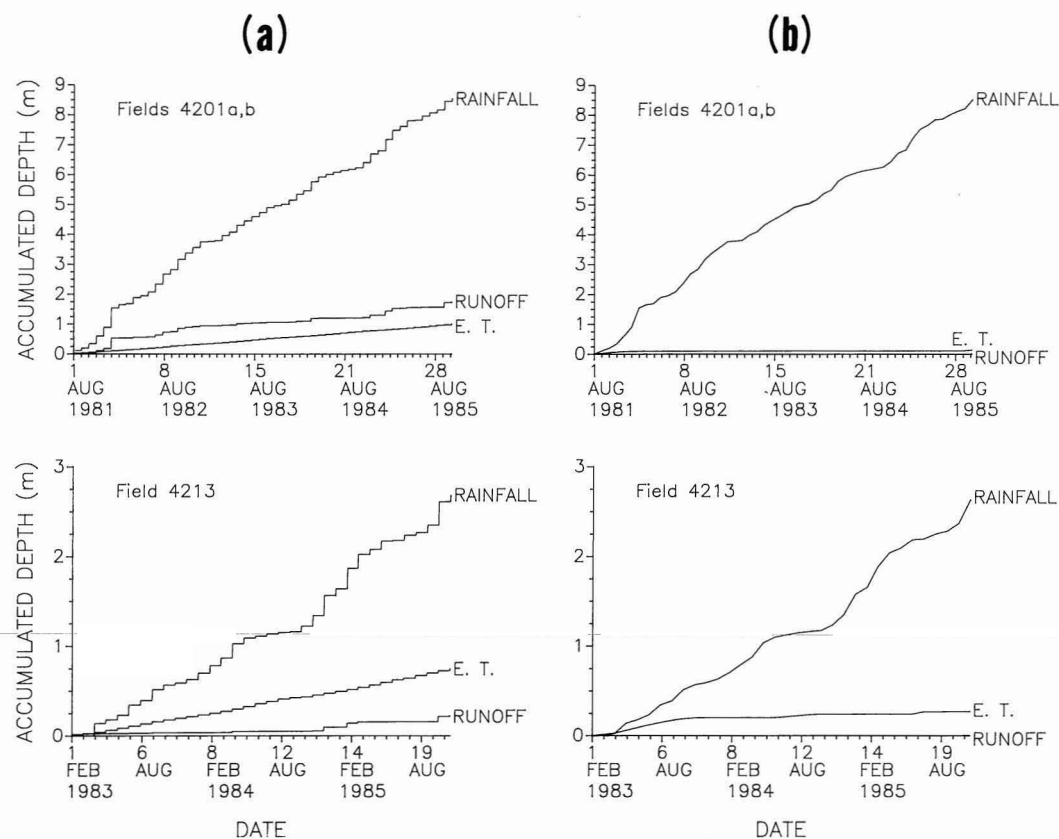


FIGURE 11. Water-balance summaries for 4201a, 4201b, and 4213 for (a) monthly rainfall and (b) daily rainfall.

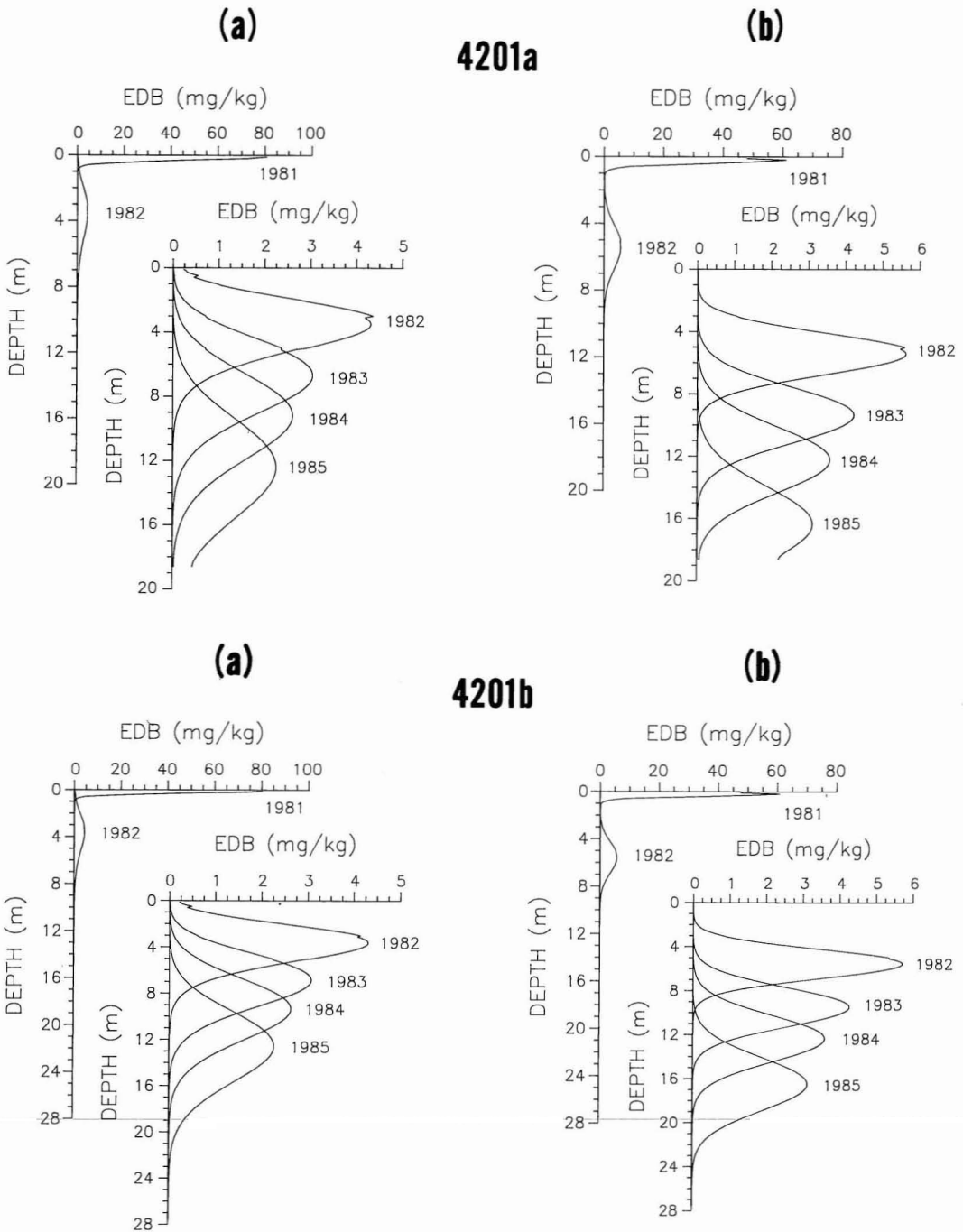


FIGURE 12. Predicted EDB concentration profiles for case A for 4201a and 4201b (above) and 4213 (facing page) for (a) monthly rainfall and (b) daily rainfall.

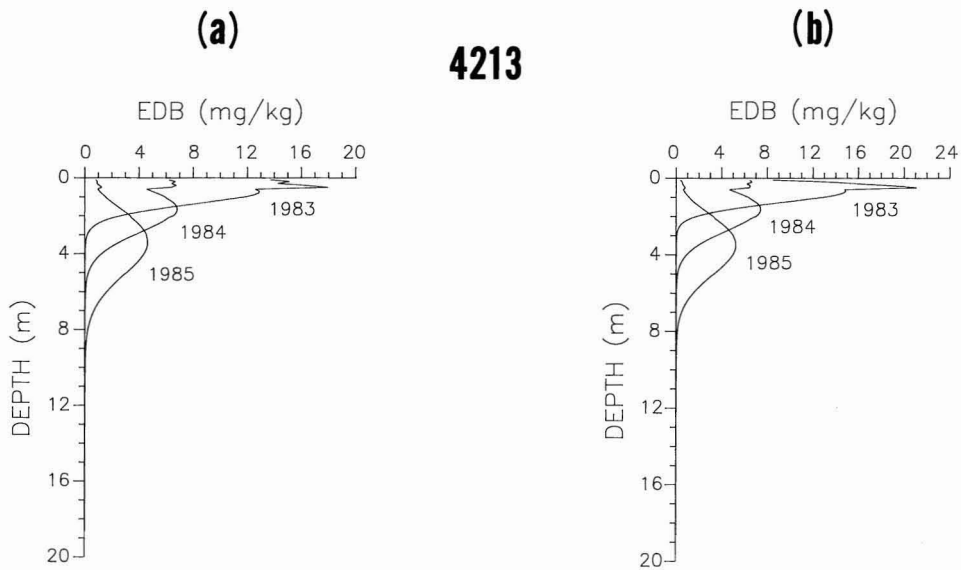


FIGURE 12 continued.

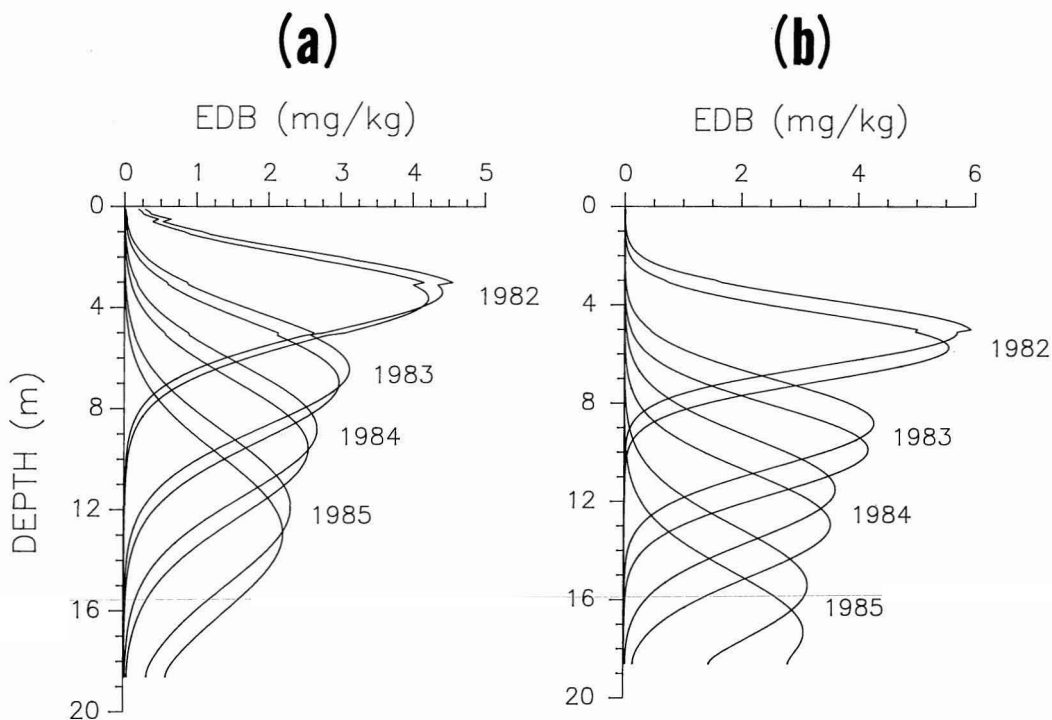


FIGURE 13. Sensitivity of predicted EDB concentration profiles for case A for 4201a for 5% changes in rainfall for (a) monthly rainfall and (b) daily rainfall.

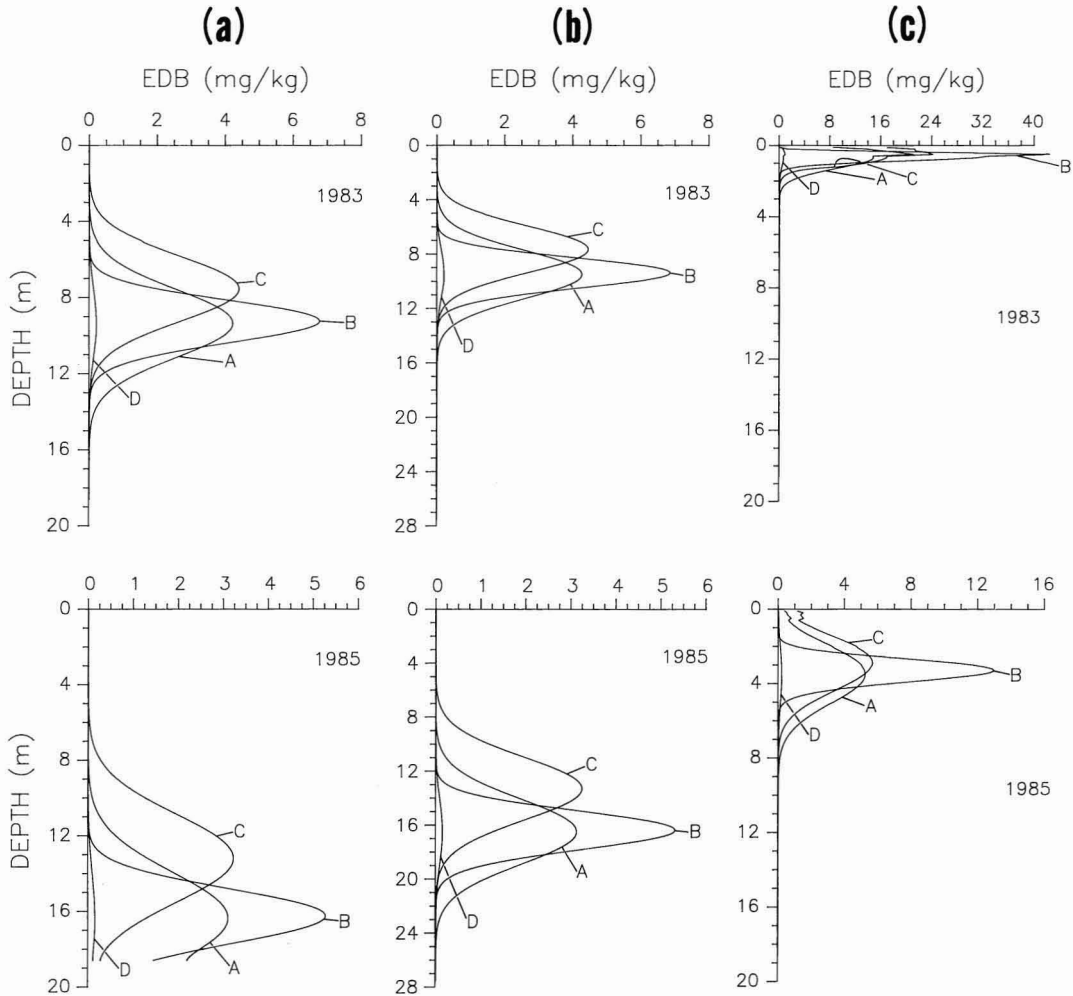


FIGURE 14. Composite overlays of predicted EDB concentration profiles for cases A–D for (a) 4201a, (b) 4201b, and (c) 4213 for the daily rainfall disaggregation scheme.

scheme. Khan and Green used temperature to estimate evapotranspiration, while in this study we used pan evaporation data. The rainfall rates and parameter values used in this study to characterize the water balance lead to surface runoff and evapotranspiration rates that are much greater for the monthly disaggregation scheme. The fact that the water-balance component of PRZM so controls the prediction of solute transport and actually can lead to paradoxical results suggests that the water-balance and disaggregation procedures

need to be critically evaluated. Although the two disaggregation techniques are equally unrealistic in terms of daily rainfall characteristics for the region (T. Giambelluca, personal communication, 1987), we have elected in the interest of space to suppress the results from monthly disaggregation in Figures 14 and 15.

(2) The effects of 5% rainfall changes (Figure 13) show that small errors in the rainfall series may significantly alter arrival times. In future work, we plan to subject PRZM to uncertainty analysis to identify the more sen-

sitive parameters and model components. We believe this exercise will produce a rationale for modifications to PRZM structure.

(3) The effect of restricted drainage (case C compared to case A, Figure 14) is a delaying shift in concentration profiles and an increase in the peak concentrations.

(4) The observed versus predicted EDB traces (Figure 15) illustrate that the uncalibrated PRZM was fairly successful in simulating the depth and time for peak concentrations but failed to represent the shape of the concentration profiles. In general, the model overpredicted concentrations by many orders of magnitude for cases A–C. The simulations that incorporated volatilization (case D) matched reality more closely as the simulation error was reduced. The reader is reminded that degradation of EDB was not considered in this study.

(5) The effect of in-field variability upon predicted EDB concentration profiles is illustrated by comparing simulations for 4201a and 4201b (Figure 12). The spatial and temporal variations for observed EDB concentration profiles are shown in Figure 4 for in-field variability (4201a and 4201b) and between-field variability (4201 and 4213).

SUMMARY AND FUTURE WORK

In this paper we have reported an initial evaluation of the suitability of PRZM for use in Hawaii. We chose to examine PRZM in an uncalibrated mode to highlight its limitations rather than perform a curve-fitting analysis. Our results suggest that PRZM can, upon modification and extension by skilled individuals, be used effectively in Hawaii. However, we feel that PRZM as it is currently structured may not be suitable for general use in Hawaii. Table 6 summarizes the confidence we have in individual model components.

We have addressed only deterministic aspects in this study. Of course, the spatial and temporal variability of rainfall, near-surface soil hydraulic properties, and chemical characteristic are knotty problems that need to be considered in the application of a model such as PRZM.

Researchers at EPA are currently modifying PRZM to improve the range of application (L. Mulkey, personal communication, 1986). EPA is also attempting to bridge PRZM to a groundwater model capable of simulating solute transport in the vadose and saturated zones (R. Swank, personal communication, 1986). There are several obvious extensions to the work reported in this paper:

(1) The disaggregation of rainfall from monthly to daily values in this study is simplistic. In future work, we plan to incorporate a more realistic disaggregation scheme.

(2) The drainage rules employed by the current version of PRZM are inappropriate for soils in Hawaii. Hawaiian soils are highly structured. We are hopeful that EPA will address the problem of preferential flow paths in future versions of PRZM.

(3) In this study, we were fortunate to have data from deep cores for three sites on two dates. In future work, we plan to use the 1983 DBCP, EDB, and TCP concentration profiles to help calibrate PRZM. It may then be possible to evaluate the predictive capabilities of the model using the 1985 observations.

(4) A number of assumptions concerning data were made in this study to excite PRZM. However, the performance of any deterministic near-surface solute-transport model such as PRZM is probably hampered most by data uncertainties. We will be in the position to improve upon many of our parameter estimates in the near future based on supplemental data we are obtaining from ongoing field measurements and laboratory analyses.

Many institutional models have been developed to simulate solute transport. However, there has been virtually no comparative evaluation of modeling techniques. As already noted, the lack of data often prevents rigorous model validation. In future work, we hope to test the limits of PRZM with synthetically generated data. The proposed data base would be created using a physically based model of the same spirit as presented in Appendix A. The input parameters for the physically based model would be described stochastically to represent various near-surface and hydrogeologic environments. The type of comparative evaluation suggested here should help to char-

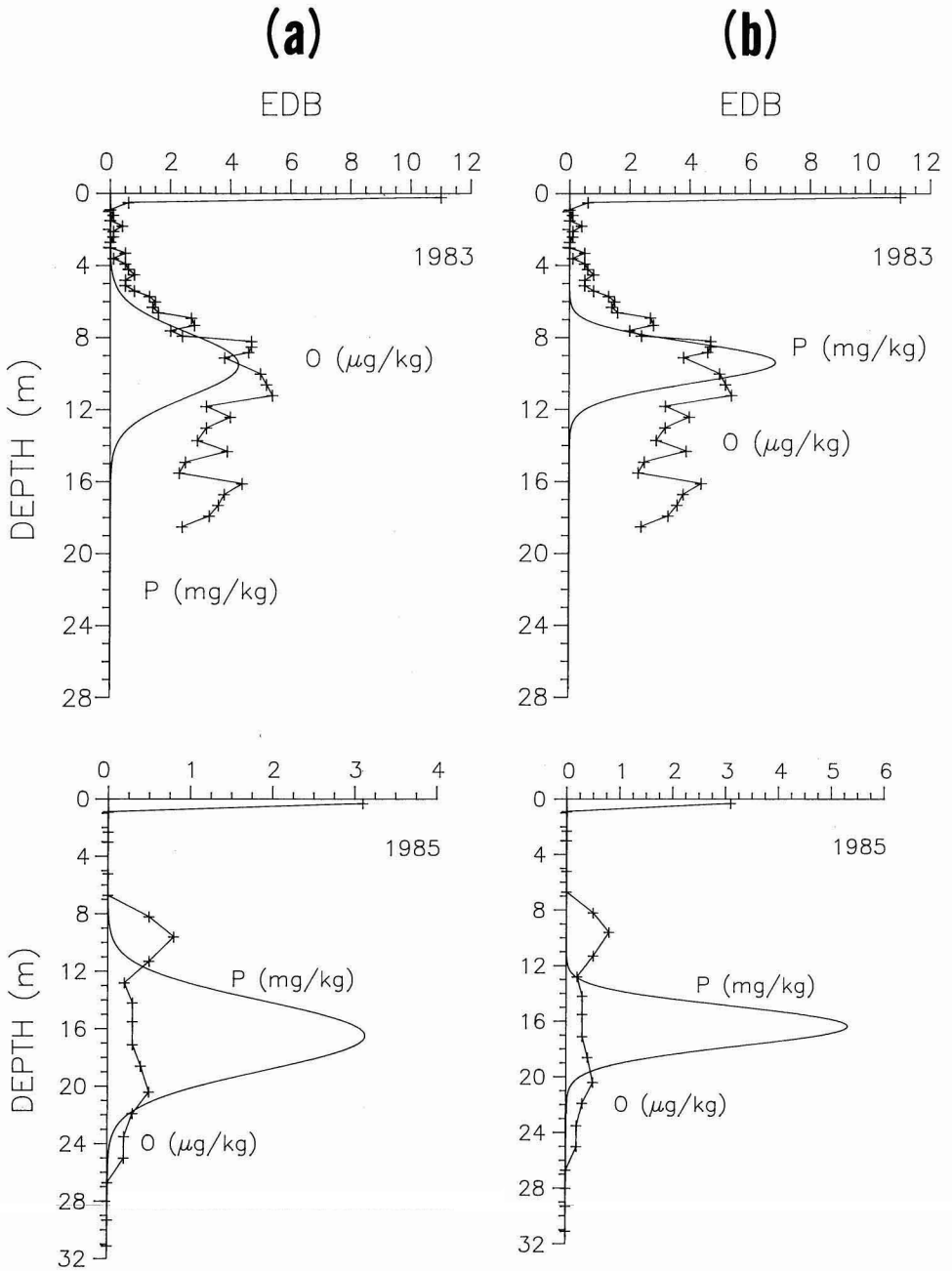


FIGURE 15. Observed (O) versus predicted (P) EDB concentration profiles for 420lb for the daily rainfall disaggregation scheme for (a) case A and (b) case B (above) and for (c) case C and (d) case D (facing page).

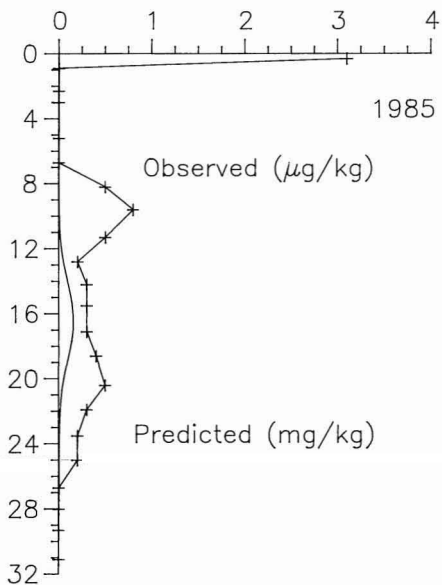
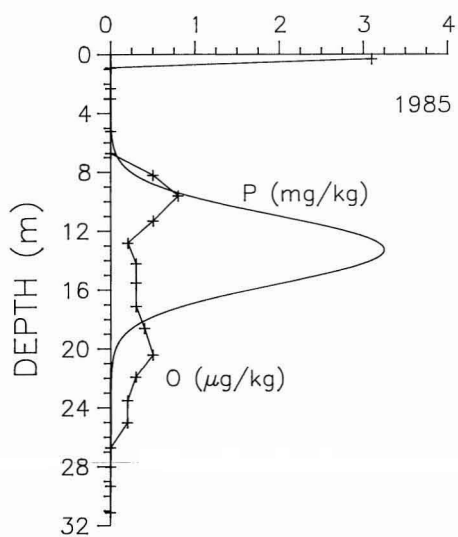
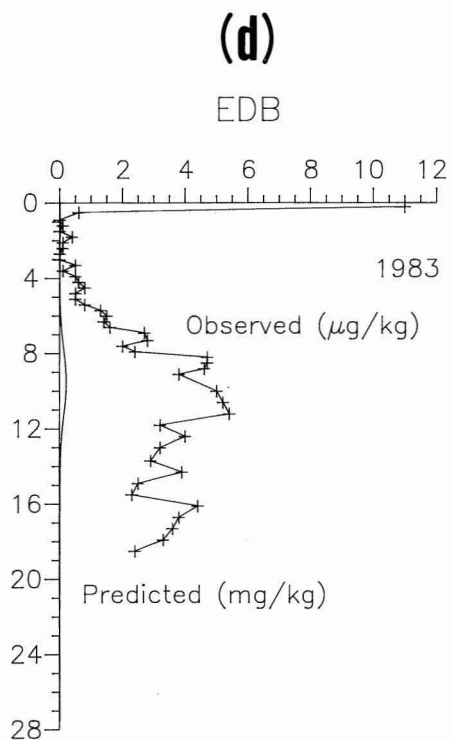
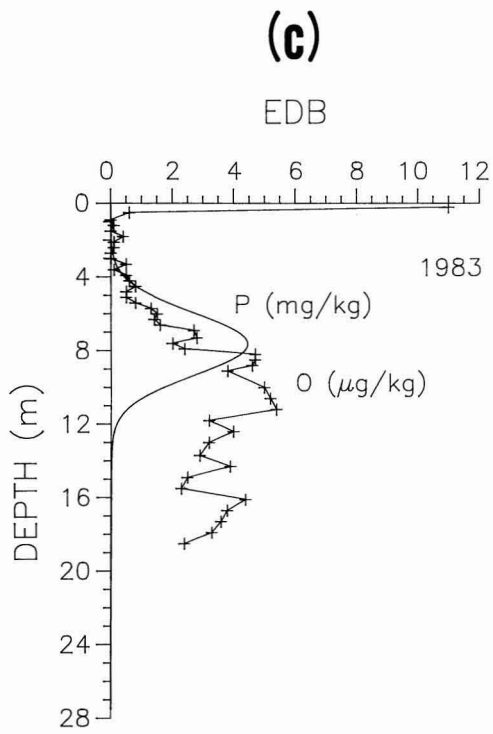


TABLE 6
SUMMARY OF PRZM COMPONENT SUITABILITIES FOR APPLICATION IN HAWAII

COMPONENT	LEVEL OF CONFIDENCE
I. Water-balance algorithm	
Interception/evapotranspiration	Moderate
Runoff	Low
Drainage	Low
II. Chemical-transport algorithm	
Advection and dispersion	Moderate
Sorption	Moderate

acterize the liabilities of using PRZM. By identifying the model components that are most vulnerable under specific conditions, it should be possible to establish guidelines for efficient use of PRZM. Such a model will help resource managers, confronted with potential groundwater contamination problems, unravel the Gordian knot associated with management decisions.

APPENDIX A

Solute-Transport Equation

The various mechanisms that control contaminant transport and attenuation in the unsaturated and saturated zones are reviewed by Nielsen et al. (1986), Yaron et al. (1984), and Freeze and Cherry (1979). In general, the movement of a solute in porous media is described by the coupled groundwater flow and advection–dispersion equations. Solute transport is a three-dimensional transient phenomenon. Most often, as in this study, pesticide transport is simulated solely in the unsaturated zone. However, groundwater contamination by agricultural chemicals does not end at the water table. In fact, the fate of these pollutants, once they reach an aquifer, is of the utmost concern. For this reason, the equations reviewed here describe unsaturated–saturated solute transport.

The three-dimensional transient unsaturated–saturated groundwater flow equation is

$$\begin{aligned} & \frac{\partial}{\partial x} \left[K_x(F, h) \frac{\partial h}{\partial x} \right] + \frac{\partial}{\partial y} \left[K_y(F, h) \frac{\partial h}{\partial y} \right] \\ & + \frac{\partial}{\partial z} \left[K_z(F, h) \left(\frac{\partial h}{\partial z} + 1 \right) \right] \quad (A.1) \\ & = \left\{ \rho g [\omega(F) + n(F)\beta] + \frac{C(F, h)}{\rho g} \right\} \frac{\partial h}{\partial t} \end{aligned}$$

where K is hydraulic conductivity (LT^{-1}), F is geologic formation or soil type, h is pressure head (L), ρ is the density of water (ML^{-3}), g is the acceleration due to gravity (LT^{-2}), ω is the coefficient of compressibility of the solid ($ML^{-1}T^{-2}$), n is porosity (dimensionless), β is the coefficient of compressibility of the fluid ($ML^{-1}T^{-2}$), C is specific water capacity (L^{-1}), x , y , z are spatial coordinates, and t is time (T).

The flow equation describes a heterogeneous anisotropic geologic environment. The pressure head solution $h(x, y, z, t)$ for the coupled unsaturated–saturated flow system can be easily converted to a hydraulic head solution $H(x, y, z, t)$ through the relationship $H = h + z$, where z is the elevation head. Solution of equation (A.1) requires knowledge of the characteristic curves $K(h)$ and $\theta(h)$. The specific water capacity $C(h)$ is the slope of the $\theta(h)$ relationship, where θ is the soil water content. The hypothetical characteristic curves in Figure A.1 illustrate that even at a small negative pressure head (h_a) the soil remains saturated. Here, h_a is known as the air entry pressure head, K^s is the saturated hydraulic conductivity, and n is the porosity. On the

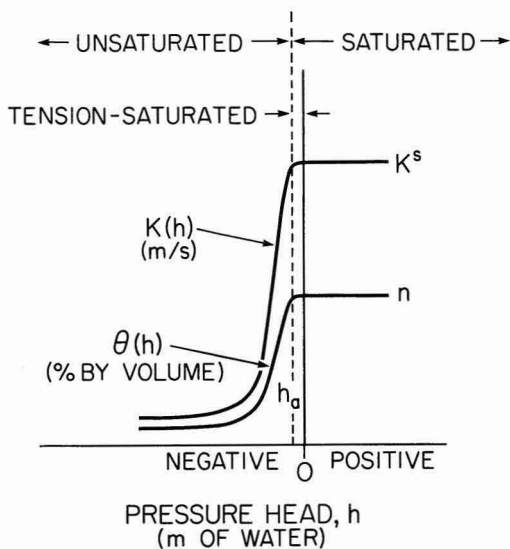


FIGURE A.1. Hypothetical characteristic curves. The $K(h)$ and $\theta(h)$ curves are further complicated by hysteretic effects; n is porosity, θ is soil water content, K^s is the saturated hydraulic conductivity, h_a is the air entry pressure head.

water table, the fluid pressure p is exactly atmospheric. Fluid pressure is related to h by the relation $p = \rho gh$; therefore, $h = 0$ on the water table. Saturated conditions exist whenever $h \geq h_a$. In the range $h_a \leq h < 0$, the pores are tension-saturated. Unsaturated conditions exist wherever $h < h_a$. Flow velocities in the x , y , and z directions in both the unsaturated and saturated regions may be calculated using Darcy's law:

$$q_x = -K_x(F, h) \frac{\partial H}{\partial x} \quad (\text{A.1a})$$

$$q_y = -K_y(F, h) \frac{\partial H}{\partial y} \quad (\text{A.1b})$$

$$q_z = -K_z(F, h) \frac{\partial H}{\partial z} \quad (\text{A.1c})$$

where q is known as the Darcy velocity.

The equation of flow described here is based on several assumptions:

1. The Darcy approach for flow through a porous medium is valid.

2. The air phase in the unsaturated zone is continuous and is at atmospheric pressure.

3. The equation is for fixed coordinates and does not consider the velocity of water with respect to the velocity of the soil grains during deformation.

4. The principal directions of anisotropy coincide with the x , y , and z coordinate axes. This reduces the nine-component second-order saturated hydraulic conductivity tensor to three components:

$$K_{ij}^s = \begin{bmatrix} K_{xx} & 0 & 0 \\ 0 & K_{yy} & 0 \\ 0 & 0 & K_{zz} \end{bmatrix} \quad \text{where } i, j = x, y, z$$

5. The fluid density is constant based on a single fluid and isothermal flow. The flow equation can be expanded to handle changing fluid density with the relationship $K = k\rho g/\mu$, where k is permeability (L^2) and μ is the dynamic viscosity of water ($ML^{-1}T^{-1}$). Both ρ and μ are functions of temperature, and k is a function of the stress-strain relationship of the porous medium.

6. The parameters g and β are system constants, and the parameters ω and n are geologic formation or soil type constants.

Of course, less ambitious versions of the flow equation than that described here are available. Various numerical solution techniques for the unsaturated-saturated flow equation are reported by Freeze (1971), Neuman (1973), and Narasimhan (1975).

The three-dimensional transient unsaturated-saturated advection-dispersion equation for a nonsorbing solute is

$$\frac{\partial}{\partial x_i} \left[\theta D_{ij}(\theta, q) \frac{\partial C_w}{\partial x_i} \right] - \frac{\partial (q_i C_w)}{\partial x_i} = \frac{\partial (\theta C_w)}{\partial t} \quad \text{where } i, j = 1, 2, 3 \quad (\text{A.2})$$

Here, θ is soil water content (dimensionless), D is dispersion tensor (L^2T^{-1}), C_w is solute concentration (ML^{-3}), and x_i are spatial coordinates. The advection-dispersion equation presented here is for a heterogeneous isotropic hydrogeologic environment. Solution takes the form $C_w(x, y, z, t)$. Water contents

$\theta(x, y, z, t)$ are a function of h and therefore can be easily evaluated from the solution of equation (A.1). The transport equation is also tied to the flow equation by the velocity terms.

The dispersion tensor is defined as

$$D_{ij} = D_{ij}^m(v, t) + D^p(\theta, t) \quad (\text{A.2a})$$

where D^m is the coefficient of mechanical dispersion and D^p is the effective liquid diffusion coefficient. The average fluid velocity v is related to the Darcy velocity by the relationship $v = q/\theta$. The coefficient of mechanical dispersion is given by

$$D_{ij}^m = \alpha_{ijmn} \frac{v_m v_n}{|v|} \quad (\text{A.2b})$$

where α_{ijmn} is the dispersivity (L), v_m and v_n are the components of the flow velocity in the m and n directions, respectively, and $|v|$ is the magnitude of the velocity vector.

The dispersivity tensor for an anisotropic porous medium is of the fourth order, with 81 components. Scheidegger (1961) shows that for an isotropic porous medium the dispersivity can be defined by longitudinal and transverse dispersivity constants. The three-dimensional second-order dispersion tensor for an isotropic porous medium has nine components:

$$D_{ij} = \begin{bmatrix} D_{xx} & D_{xy} & D_{xz} \\ D_{yx} & D_{yy} & D_{yz} \\ D_{zx} & D_{zy} & D_{zz} \end{bmatrix}$$

Inspection of equations (A.2a) and (A.2b) suggests that at higher velocities dispersion will be controlled by D^m , while at lower velocities D^p will dominate.

The advection–dispersion equation described here is based on many assumptions, including the following:

1. Dispersion in porous material is Fickian.
2. The dispersivity tensor is symmetrical (the medium is isotropic) and has its principal direction aligned with the velocity vector.
3. Dispersion in partially saturated media follows the theory developed for saturated flow.

The advection–dispersion equation as presented here can be expanded to include the

effects of chemical and biological reactions within the unsaturated–saturated flow system. These reactions include volatilization, sorption–desorption, biological degradation, plant uptake, chemical decay, oxidation–reduction, and precipitation–dissolution. The mathematical relationships that describe these processes enjoy different levels of rigor. Each new component added to the advection–dispersion equation requires additional parameters and increases the number of underlying assumptions upon which the model is based.

The coupled numerical solution of equations (A.1) and (A.2) comprise what we shall refer to as a “physically based model.” The model is a deterministic conceptual representation of solute-transport processes.

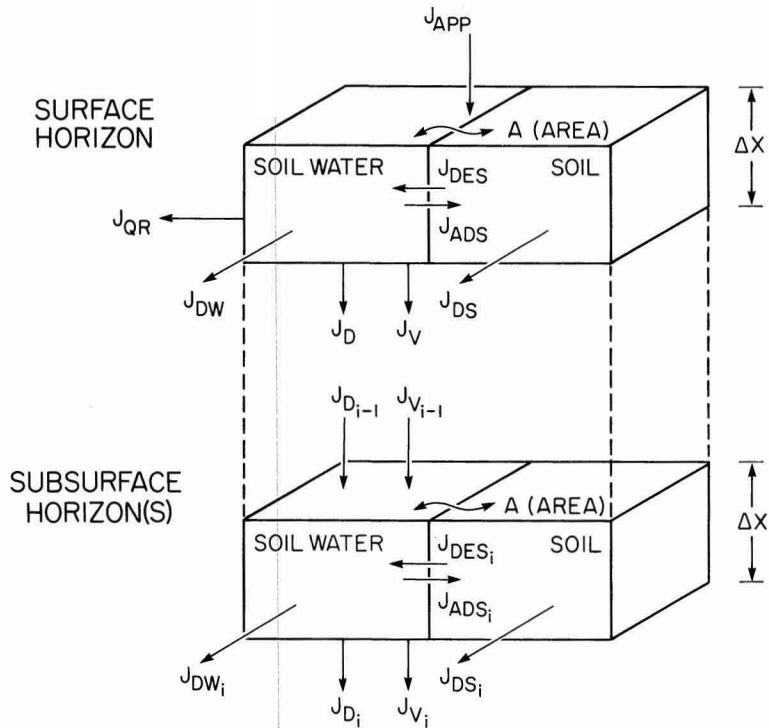
Davis and Segol (1985) and Voss (1984) each describe models that simulate fluid flow and solute transport in unsaturated–saturated porous media. The utility of physically based models for field problems is often restricted by staggering data requirements and computer capacity limitations. The physically based model described here, although certainly not the end of the theoretical rainbow, is probably most useful for the development of concepts and testing of simpler models. Our objective in presenting the physically based model here has been to set a standard to which the reader can compare the less rigorous PRZM described in the main body of the paper and in Appendix B.

APPENDIX B

Pesticide Root Zone Model (PRZM)

PRZM uses a compartmentalized design to simulate one-dimensional vertical chemical movement in unsaturated soil systems near the soil surface. The structure of PRZM, as utilized in this study, is based upon the soil profile representation shown in Figure B.1. The discussion in this section is a summary of the second chapter of Carsel et al. (1984).

The mass balance equations for the surface zone in Figure B.1 are



ΔX = COMPARTMENT SIZE

J_{ADS} = ADSORPTION

J_{APP} = APPLICATION

J_D = DISPERSION

J_{DES} = DESORPTION

J_{DS} = DECAY-SOIL

J_{DW} = DECAY-WATER

J_{QR} = RUNOFF

J_V = ADVECTION

1. Mass flow due to advection and dispersion-diffusion, $J_{D,V}$ and J_{D_i,V_i}

$J_{D,V}$ = Flow across upper boundary of compartment

J_{D_i,V_i} = Flux across lower boundary of compartment

Assume: Dispersive-diffusive term is constant

2. Reversible Sorption, J_{ADS} , J_{DES} and J_{ADS_i} , J_{DES_i}

J_{ADS} = Adsorption of chemical to soil

J_{DES} = Desorption of chemical from soil

Assume: Equilibrium between phases is reached instantaneously

3. Chemical Decomposition, J_{DW} , J_{DS} and J_{DW_i} , J_{DS_i}

J_{DW} = Decay in the soil water phase

J_{DS} = Decay in the soil phase

Assume: One first order decomposition rate represents the sum of all processes in both soil water and soil phases

FIGURE B.1. Compartmental model for pesticide transport in soil as used in this study (adapted from Carsel et al. 1984).

$$J_{APP} + J_{DES} - J_{ADS} - J_{QR} - J_{DW} - J_v - J_D = \frac{A\Delta X \partial(C_w \theta)}{\partial t} \quad (\text{B.1a})$$

$$J_{ADS} - J_{DES} - J_{DS} = \frac{A\Delta X \partial(C_s \rho_s)}{\partial t} \quad (\text{B.1b})$$

where A is cross-sectional area of soil column (L^2), ΔX is depth dimension of compartment (L), C_w is dissolved concentration of pesticide (ML^{-3}), C_s is sorbed concentration of pesticide (dimensionless), θ is volumetric water content of soil (dimensionless), ρ_s is soil bulk density (ML^{-3}), t is time (T), J_D is mass rate of change by dispersion (MT^{-1}), J_v is mass rate of change by advection (MT^{-1}), J_{DW} is mass rate of change by transformation of dissolved phase (MT^{-1}), J_{QR} is mass rate of change by removal in runoff (MT^{-1}), J_{APP} is mass rate of change by pesticide application (MT^{-1}), J_{DS} is mass rate of change by transformation of sorbed phase (MT^{-1}), J_{ADS} is mass rate of change by adsorption (MT^{-1}), and J_{DES} is mass rate of change by desorption (MT^{-1}). Mass balance relations for the subsurface are identical to the surface except for the runoff term.

The PRZM water-balance algorithm for this study is given by

Surface ($i = 1$):

$$\theta_i^{t+1} = \theta_i^t + P - Q - I_i - E_i \quad (\text{B.2a})$$

Root zone ($i = 2, n$; n is the bottom of the root zone):

$$\theta_i^{t+1} = \theta_i^t + I_{i-1} - I_i - U_i \quad (\text{B.2b})$$

Below root zone ($i = n + 1, m$; m is the bottom of the soil profile):

$$\theta_i^{t+1} = \theta_i^t + I_{i-1} - I_i \quad (\text{B.2c})$$

where θ_i^t is soil water content in layer i of the noted zone on day t (L), P is rainfall minus interception (LT^{-1}), Q is runoff (LT^{-1}), E_i is evaporation (LT^{-1}), U_i is transportation (LT^{-1}), and I_i is percolation out of zone i (LT^{-1}).

Runoff estimates with PRZM are based upon a curve number approach,

$$Q = \frac{(P - 0.2R)^2}{P + 0.8R} \quad (\text{B.3})$$

where R is a retention parameter (dimensionless). The retention parameter is estimated by the expression $R = 1000/CN - 10$, where CN (dimensionless) is the curve number that is a function of soil type, drainage properties, crop type, and management practice. In PRZM, curve numbers are determined each day as a function of soil water status in the upper soil layers.

The daily evapotranspiration (ET) is divided among evaporation from canopy, soil evaporation, and crop transpiration. Total demand is first estimated and then extracted sequentially from crop canopy storage and from each layer until wilting point is reached in each layer or until total demand is met. Evaporation occurs down to a user-specified depth. The remaining demand, crop transpiration, is met from the layers between this depth and active rooting depth. The actual evapotranspiration demand is estimated as

$$ET_i = \text{Min} \left[(\theta_i^t - \theta_i^{wp}) f_{di}; ET_p - \sum_1^{i-1} ET_i \right] \quad (\text{B.4})$$

where ET_i is actual evapotranspiration from layer i (L), f_{di} is the depth factor for layer i (dimensionless), θ_i^{wp} is wilting point soil water content in layer i (L), and ET_p is potential evapotranspiration (L). The depth factor linearly weights the extraction of ET from the root zone with depth in a triangular fashion.

Evapotranspiration is also limited by soil water availability. The potential rate may not be met if sufficient soil water is not available to meet the demand; PRZM modifies the potential by the following equations:

$$ET_p = ET_p \quad \text{if } \theta^t \geq 0.6 \theta^{fc} \quad (\text{B.5a})$$

$$ET_p = \text{SMFAC} \cdot ET_p \quad \text{if } \theta^{wp} < \theta^t < 0.6 \theta^{fc} \quad (\text{B.5b})$$

$$ET_p = 0 \quad \text{if } \theta^t \leq \theta^{wp} \quad (\text{B.5c})$$

where θ^{fc} is soil water content at field capacity (dimensionless) and SMFAC is a soil water factor (dimensionless). The SMFAC parameter is internally set in the code to reduce ET_p linearly according to the limits imposed in the above equations. Finally, ET_p is estimated from pan evaporation as $ET_p = C_p \cdot PE$, where

PE (LT^{-1}) is pan evaporation and C_p (dimensionless) is the pan factor. The pan factor is constant for a given location and is a function of the average daily relative humidity, average daily windspeed, and location of the pan with respect to an actively transpiring crop.

The final term in the water-balance equations is percolation. The use of the SCS curve number approach for runoff precludes the direct use of a Darcy model for simulating unsaturated flow. As described in the main body of the paper, PRZM resorts to drainage rules keyed to soil water storages and the time available for drainage. The drainage rules are simplistic but consistent with the intent of the model.

A decoupled approach is taken for simulating solute transport with PRZM. Pore water velocities are estimated from the percolation terms in the water balance rather than from Richard's equation. The velocity estimates are subsequently passed to a finite-difference approximation of the one-dimensional advection-dispersion equation. The spatial increments of the transport equation are the same as those used in the water-balance calculations. The reader is reminded that a coupled, physically based approach for solute-transport simulation is described in Appendix A.

Sorption and desorption are treated as separate kinetic processes by PRZM. The linear relationship used for both sorption and desorption is presented in the main body of the paper. Degradation processes such as hydrolysis, photolysis, and microbial decay are assumed, with the use of PRZM, to follow pseudo first-order kinetics and therefore yield rate coefficients that may be combined into sorbed and dissolved phase decay coefficients. The degradation component of PRZM was not used in the work reported here, but is currently being utilized in our ongoing investigation. The reader interested in a more comprehensive treatment of PRZM is directed to Carsel et al. (1984).

ACKNOWLEDGMENTS

We are indebted to many organizations, both public and private, for their selfless shar-

ing of information. The cooperation of Lyle Wong, Tom Giambelluca, and Paul Ekern is greatly appreciated.

LITERATURE CITED

- ANDERSON, M. P. 1979. Using models to simulate the movement of contaminants through groundwater flow systems. *CRC critical reviews*. Environ. Contr. 9(2):97-156.
- BUSH, P. B., J. F. DOWD, D. G. NEARCY, and W. L. NUTTER. 1985. Application of PRZM to pesticide movement in a forested watershed. *Agron. Abstr.* 216.
- CARSEL, R. F., W. B. NIXON, and L. G. BALLANTINE. 1986. Comparison of pesticide root zone model predictions with observed concentrations for the tobacco pesticide metalaxyl in unsaturated zone soils. *Environ. Toxicol. Chem.* 5:345-353.
- CARSEL, R. F., L. A. MULKEY, M. H. LORBER, and L. B. BASKIN. 1985. The pesticide root zone model (PRZM): A procedure for evaluating pesticide leaching threats to groundwater. *Ecol. Model.* 30:49-69.
- CARSEL, R. F., C. H. SMITH, L. A. MULKEY, J. D. DEAN, and P. P. JOWISE. 1984. User's manual for the pesticide root zone model: Release 1. U.S. Environmental Protection Agency, EPA-600/3-84-109.
- COOLEY, K. R., and L. J. LANE. 1982. Modified runoff curve numbers for sugarcane and pineapple fields in Hawaii. *J. Soil Water Conserv.* 37(5):295-298.
- DAVIS, L. A., and G. SEGOL. 1985. Documentation and user's guide: GS2 and GS3—variably saturated flow and mass transport models. U.S. Nuclear Regulatory Commission, Final Rept. NUREG/CR-3901.
- DEAN, J. D., P. P. JOWISE, and A. S. DONIGIAN, JR. 1984. Leaching evaluation of agricultural chemicals (LEACH) handbook. U.S. Environmental Protection Agency, EPA-600/3-84-068.
- DIVISION OF WATER AND LAND DEVELOPMENT. 1973. Climatologic stations in Hawaii. Dept. of Land and Natural Resources, Rept. R72. State of Hawaii, Honolulu.
- EKERN, P. C. 1965. Evapotranspiration of

- pineapple in Hawaii. *Plant Physiol.* 40: 736-739.
- EKERN, P. C. and J. H. CHANG. 1985. Pan evaporation: State of Hawaii, 1894-1983. Dept. of Land and Natural Resources, Rept. R74. State of Hawaii, Honolulu.
- EPSTEIN, S. S., L. O. BROWN, and C. POPE. 1982. Hazardous waste in America. Sierra Club Books, San Francisco, Ca.
- FREEZE, R. A. 1971. Three-dimensional transient, saturated-unsaturated flow in a groundwater basin. *Water Resources Res.* 7(2):347-366.
- FREEZE, R. A., and J. A. CHERRY. 1979. Groundwater. Prentice Hall, Englewood Cliffs, N.J.
- GIAMBELLUCA, T. W. 1987. Influence of time interval size on water-balance computations. Paper, Ann. Meet. Assoc. Amer. Geogr., April 21-26, Portland, Ore.
- GIAMBELLUCA, T. W., and D. S. OKI. 1987. Temporal disaggregation of monthly rainfall data for water-balance modeling. Paper, IUGG/IAHS Gen. Assembly, Aug. 9-22, Univ. of British Columbia, Vancouver, B.C., Canada.
- GIAMBELLUCA, T. W., M. A. NULLET, and T. A. SCHROEDER. 1986. Rainfall atlas of Hawaii. Dept. of Land and Natural Resources, Rept. R76. State of Hawaii, Honolulu.
- GREEN, R. E., and S. W. KARICKHOFF. 1988. Estimating pesticide sorption coefficients for soils and sediments. Vol. III. Small watershed model ARS/USDA (in press).
- GREEN, R. E., C. C. K. LIU, and N. TAMRAKAR. 1986. Modeling pesticide movement in the unsaturated zone of Hawaiian soils under agricultural use. Pages 366-383 in W. Y. Garner, R. C. Honeycutt, and H. N. Nigg, eds. Evaluation of pesticides in groundwater. Amer. Chem. Soc. Symp. Ser. 315. American Chemical Society, Washington, D.C.
- GREEN, R. E., L. R. AHUJA, S. K. CHONG, and L. S. LAU. 1982. Water conduction in Hawai'i oxic soils. Water Resources Research Center, University of Hawaii at Manoa, Techn. Rept. 143.
- JONES, R. L. 1983. Movement and degradation of aldicarb residues in soil and water. Paper, Environ. Toxicol. Chem. Conf. Multidisciplinary Approaches to Environ. Probl., Nov. 6-9, Crystal City, Va.
- JONES, R. L., P. S. C. RAO, and A. G. HORNSBY. 1983. Fate of aldicarb in Florida citrus soil. 2: Model evaluation. Paper, Conf. Characterization and Monitoring of the Vadose (Unsaturated) Zone. Dec. 8-10, Las Vegas, Nev.
- KHAN, M. K., and R. E. GREEN. 1988. Use of the pesticide root zone model (PRZM) for assessing DBCP leaching in Hawaii. Hawaii Inst. Trop. Agric. Hum. Res. Ser. 054. University of Hawaii, Honolulu.
- LAU, L. S., and J. F. MINK. 1987. Organic contamination of groundwater: A learning experience. *J. Amer. Water Well Assoc.* 79(8):37-42.
- MELANCON, S. M., J. E. POLLARD, and S. C. HERM. 1986. Evaluation of SESOIL, PRZM and PESTAN in a laboratory column leaching experiment. *Environ. Toxicol. Chem.* 5:865-878.
- NARASIMHAN, T. N. 1975. A unified numerical model for saturated groundwater flow. Ph.D. Thesis. University of California, Berkeley.
- NEUMAN, S. P. 1973. Saturated-unsaturated seepage by finite elements. *J. Hydraulic Div. ASCE* 99 (HY12):2233-2250.
- NIELSEN, D. R., M. T. VAN GENUCHTEN, and J. W. BIGGAR. 1986. Water flow and solute-transport processes in the unsaturated zone. *Water Resources Res.* 22(9):895-1085.
- OKI, D. S., and T. W. GIAMBELLUCA. 1985. Subsurface water and soil quality data base for State of Hawaii: Part 1. Water Resources Research Center, University of Hawaii at Manoa, Spec. Rept. 7.
- OR, S. 1987. Multiple-cell simulation of trace organics transport in balsaltic aquifer, southern Oahu, Hawaii. M.S. Thesis. University of Hawaii, Manoa.
- PETERSON, F. L., K. R. GREEN, R. E. GREEN, and J. N. OGATA. 1985. Drilling program and pesticide analysis of core samples from pineapple fields in central Oahu. Water Resources Research Center, University of Hawaii at Manoa, Spec. Rept. 7.5 (unpublished).

- PYE, V. I., and R. PATRICK. 1983. Groundwater contamination in the United States. *Science* 221:713–718.
- SCHEIDEGGER, A. E. 1961. General theory of dispersion in porous media. *J. Geophys. Res.* 66:3273–3278.
- SUN, M. 1986. Groundwater ills: Many diagnoses, few remedies. *Science* 232:1490–1493.
- U.S. SOIL CONSERVATION SERVICE. 1976. Soil survey laboratory data and descriptions for some soils of Hawaii. Soil Survey Investigations Rept. 29.
- VOSS, C. I. 1984. SUTRA: A finite-element simulation model for saturated–unsaturated, fluid density-dependent groundwater flow with energy transport or chemically reactive single-species solute transport. Water Resources Investigations Rept. 84-4369. U.S. Geological Survey National Center, Reston, Va.
- WONG, L. 1983. Preliminary report on soil sampling EDB on Oahu. Pesticide Branch, Div. of Plant Industry, Dept. of Agriculture, State of Hawaii (unpublished).
- . 1987. Analysis of ethylene dibromide distribution in the soil profile following shank injection for nematode control in pineapple culture. Pages 28–40 in P.S.C. Rao and R. E. Green, eds. Toxic organic chemicals in Hawaii's water resources. Hawaii Inst. Trop. Agric. Hum. Resources Res. Exten. Ser. 086. University of Hawaii, Honolulu.
- YARON, B., G. DAGON, and J. GOLDSHMID, eds. 1984. Pollutants in porous media. Springer-Verlag, New York.